

# Shape Matching by Variational Computation of Geodesics on a Manifold\*

Frank R. Schmidt, Michael Clausen, and Daniel Cremers

Department of Computer Science  
University of Bonn  
Römerstr. 164, 53117 Bonn, Germany  
{schmidtf, clausen, dcremers}@cs.uni-bonn.de

**Abstract.** Klassen et al. [9] recently developed a theoretical formulation to model shape dissimilarities by means of geodesics on appropriate spaces. They used the local geometry of an infinite dimensional manifold to measure the distance  $\text{dist}(A, B)$  between two given shapes  $A$  and  $B$ . A key limitation of their approach is that the computation of distances developed in the above work is inherently unstable, the computed distances are in general not symmetric, and the computation times are typically very large. In this paper, we revisit the shooting method of Klassen et al. for their angle-oriented representation. We revisit explicit expressions for the underlying space and we propose a gradient descent algorithm to compute geodesics. In contrast to the shooting method, the proposed variational method is numerically stable, it is by definition symmetric, and it is up to 1000 times faster.

## 1 Introduction

The modeling of shapes and distances between shapes is one of the fundamental problems in Computer Vision with applications in the fields of image segmentation, tracking, object recognition, and video indexing. In recent years, a considerable amount of effort has been put into the understanding of closed planar curves modulo some transformations, which will be referred to as shapes. To measure the dissimilarity between two given shapes requires the definition and examination of metric spaces which model shapes (cf. [7,4,5,1]).

In 2003, Michor and Mumford [11] described a way to define a shape space using manifolds. The distance between two given shapes were defined as the minimal length of a path  $m$  on the manifold connecting these shapes. Such paths are known as *geodesics*. The model is presented in a very general fashion, i.e., in order to calculate geodesics on this manifold, a partial differential equation (PDE) has to be solved. Hence, it is not suitable for online-calculation to find the shortest geodesic between two given shapes.

In the same year, Klassen et al. also presented metric spaces using manifolds [9].<sup>1</sup> Their model is focused on closed planar curves parametrized by arclength.

\* This work was supported by the German Research Foundation, grant #CR-250/1-1.

<sup>1</sup> For an extension of the notion of geodesics to closed curves embedded in  $\mathbb{R}^3$  we refer to [8].

This simplification led to an ordinary differential equation (ODE) instead of a PDE for the geodesic-calculation. Moreover, the calculation of the shortest geodesic could in many cases be done within seconds using the so called *shooting method*. This method uses a searching beam from the initial shape. That beam will be changed until the target shape is found, where the beam is deformed according to the underlying metric just as a light beam is bent by gravity in the theory of general relativity.

In this paper, we will use the same manifold that was introduced in [9]. But we will abandon the shooting method and replace it by a *variational method* which is more stable, by definition symmetric and allows a faster algorithm than the algorithm introduced by Klassen et al. This variational method is a gradient descent method with respect to the energy functional  $E(m) := \int_0^1 \langle m'(t), m'(t) \rangle_{m(t)} dt$ .

This paper is organized as follows. In Section 2 we revisit the shape space and a toolbox of helpful functions that were presented in [9]. In Section 3 we review the shooting method and introduce an alternative variational method to calculate geodesics on the shape space. In Section 4 we compare both methods with special interest on correctness, accuracy and computation time. In Section 5 we provide a conclusion.

## 2 Modeling Shapes

Given any smooth closed planar contour  $\Gamma \subset \mathbb{C}$ , the group of translations, rotations and uniform scalings creates a family  $[\Gamma]$  of closed planar contours. The elements of this family have all one property in common - *their shape*. Therefore, we will consider the set of all such families and call this set the shape space. In this section, we will revisit a manifold that was proposed in [9] to handle this shape space. We are especially interested in morphings, i.e., smooth short transformations from one given shape to another. On the manifold, these morphings will be described by geodesics [6,3]. Hence, on the shape space a metric is induced which provides a measure of the dissimilarity of two given shapes.

### 2.1 Manifold of Preshapes

To model shapes, we consider closed planar curves that are parametrized via the unit circle  $\mathbb{S}^1 = \{x \in \mathbb{C} \mid \|x\| = 1\}$ . A closed planar curve is therefore a  $C^\infty$ -mapping  $c : \mathbb{S}^1 \rightarrow \mathbb{C}$  with a non-vanishing derivative  $c'$ . Because the derivative of the mapping  $c$  ignores translation of the contour  $\Gamma$ , we will consider  $c'$  instead of  $c$ . To get rid of possible scalings, we fix the length of  $\Gamma$  by  $2\pi$ . This can be achieved by modeling any shape via curves  $c : \mathbb{S}^1 \rightarrow \mathbb{C}$  that are *parametrized by arclength*. Thus,  $c' : \mathbb{S}^1 \rightarrow \mathbb{S}^1$  can be modeled via a  $C^\infty$ -mapping  $\vartheta : [0; 2\pi] \rightarrow \mathbb{R}$  which realizes the following lifting-equations  $c'(e^{it}) = e^{i\vartheta(t)}$  and  $\vartheta(2\pi) = \vartheta(0) + 2\pi$ . This mapping  $\vartheta$  is unique up to addition of a constant  $2\pi\ell$ ,  $\ell \in \mathbb{Z}$ . Moreover, the addition of any  $r \in \mathbb{R}$  to  $\vartheta$  is equivalent to a rotation of  $c$  by the angle  $r$ . These observations lead to the manifold<sup>2</sup>  $\mathcal{C} := \Psi^{-1}((2\pi^2, 0, 0)^\top) \subset L^2 := L^2([0; 2\pi], \mathbb{R})$ ,

<sup>2</sup> In [9], two different manifolds were presented. We will restrict ourselves to the manifold that handles the angle-oriented mapping  $\vartheta$ .

$$\Psi(\vartheta) := \left( \int_0^{2\pi} \vartheta(\tau) d\tau, \int_0^{2\pi} \sin(\vartheta(\tau)) d\tau, \int_0^{2\pi} \cos(\vartheta(\tau)) d\tau \right)^\top.$$

As it was outlined in [9], this manifold  $\mathcal{C}$  does not describe the shape space. Moreover, one shape  $[I]$  can possess multiple representations in this so called preshape space  $\mathcal{C}$ . To be specific, for any  $\alpha \in \mathbb{R}$  the mappings  $c : t \mapsto c(e^{it})$  and  $c_\alpha : t \mapsto c(e^{i(t+\alpha)})$  describe the same closed planar contour  $I \subset \mathbb{C}$ . Let  $\vartheta$  and  $\vartheta_\alpha$  be the lifting representation for  $c$  resp.  $c_\alpha$ . Then, the set  $\{\vartheta_\alpha | \alpha \in [0; 2\pi[ \} =: \vartheta \cdot \mathbb{S}^1 \subset \mathcal{C}$  contains all different representations of  $\vartheta$  within  $\mathcal{C}$  that describe the same shape (cf. Figure 1). The notation  $\vartheta \cdot \mathbb{S}^1$  is motivated by the fact that

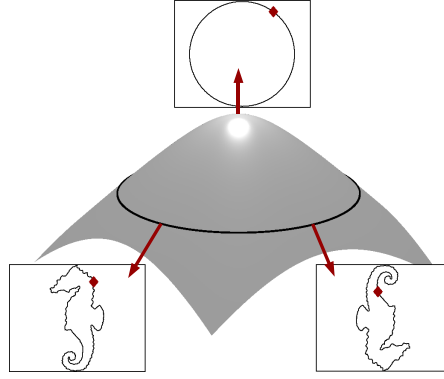


**Fig. 1.** Since any shape can be parametrized with differing starting points, it corresponds to a family of preshapes which form a closed curve on the manifold of preshapes. Symmetries of a given shape will be reflected by multiple coverings of this curve. In the case of a circle, this preshape curve will collapse to a single point.

$\alpha \mapsto \vartheta_\alpha$  is a group operation with at least  $2\pi\mathbb{Z}$  as stabilizer. The shape space  $\mathcal{S} := \mathcal{C}/\mathbb{S}^1$  consists of all orbits  $\vartheta \cdot \mathbb{S}^1 \subset \mathcal{C}$  [9]. Therefore, any metric  $\text{dist}_{\mathcal{C}}$  on  $\mathcal{C}$  induces the metric

$$\text{dist}_{\mathcal{S}}(\vartheta_1 \cdot \mathbb{S}^1, \vartheta_2 \cdot \mathbb{S}^1) := \min_{s_1 \in \mathbb{S}^1} \min_{s_2 \in \mathbb{S}^1} \text{dist}_{\mathcal{C}}(\vartheta_1 \cdot s_1, \vartheta_2 \cdot s_2) \quad (1)$$

on  $\mathcal{S}$ . In the next section, we will discuss the metric on any manifold  $M$  that is induced by geodesics. This geodesic metric will be used as  $\text{dist}_{\mathcal{C}}$  and thus, induces  $\text{dist}_{\mathcal{S}}$  via (1).

## 2.2 Geodesics on Manifolds

In this section, we will present the idea of geodesics and two different ways to calculate geodesics. Let  $\mathbb{E}$  be a Euclidean  $k$ -dimensional vector space (e.g.,  $\mathbb{R}^k \subset \mathbb{R}^n$ ).  $E$  possesses a scalar product denoted by  $\langle \cdot, \cdot \rangle$ . Using this product, the length of any smooth path  $m : [0; 1] \rightarrow \mathbb{E}$  is  $\text{len}(m) := \int_0^1 \langle m'(t), m'(t) \rangle^{\frac{1}{2}} dt$ . The

distance of two arbitrary points  $x, y \in \mathbb{E}$  can be defined as the minimal length of smooth paths that connect these two points, i.e.,  $m(0) = x$  and  $m(1) = y$ . To any path  $m$ , there exists a path  $\tilde{m}$  of same image and length that is parametrized by arclength. Moreover, every path of minimal length that is parametrized by arclength also minimizes the energy-functional  $E(m) := \int_0^1 \langle m'(t), m'(t) \rangle dt$ . In the case of  $\mathbb{E} = \mathbb{R}^k$ , the Euler-Lagrange equation becomes  $0 \equiv \frac{d}{dt} m' \equiv m''$ . Paths which realize this equation are called *geodesics*.

Now, consider any embedded  $k$ -dimensional manifold  $M \subset \mathbb{R}^n$ , e.g., a sphere or a cylinder. At any point  $x \in M$  there exists the  $k$ -dimensional tangent space  $T_x M$ . On this tangent space the scalar product of  $\mathbb{R}^n$  induces a scalar product denoted by  $\langle \cdot, \cdot \rangle_x$ . Given any smooth path  $m: [0; 1] \rightarrow M$ , the *length* of this path can be calculated by  $\text{len}(m) := \int_0^1 \langle m'(t), m'(t) \rangle_{m(t)}^{\frac{1}{2}} dt$ . Analogously to the Euclidean space, geodesics can be defined and a geodesic equation can be found. In the Euclidean case,  $m'$  and  $m''$  are  $k$ -dimensional vector fields along  $m$ . In the case of a manifold, only  $m'$  is a  $k$ -dimensional vector field, i.e.,  $m'(t) \in T_{m(t)} M$ . On the other hand,  $m''$  is an  $n$ -dimensional vector field that can be split into a tangential ( $k$ -dimensional) vector field  $m''^{\text{tan}}$  and a normal vector field  $m''^{\text{nor}}$ . With this notations the geodesic equation becomes  $0 \equiv m''^{\text{tan}}$ . Given a starting point  $x \in M$  and a starting direction  $v \in T_x M$ , the following differential equation

$$m(0) = x \qquad m'(0) = v \qquad m''^{\text{tan}}(t) \equiv 0$$

can be uniquely solved by a path  $m_{x,v}: \mathbb{R} \rightarrow M$ . This property leads to the definition of the so called exponential mapping  $\exp_x(v) := m_{x,v}(1)$ . Using this mapping, the distance of two arbitrary points  $x, y \in M$  is

$$\text{dist}_M(x, y) := \min_{\substack{m \text{ smooth path,} \\ m(0) = x, m(1) = y}} \text{len}(m) = \min_{\substack{v \in T_x M: \\ y = \exp_x(v)}} \langle v, v \rangle_x^{\frac{1}{2}}. \quad (2)$$

While the shooting method used in [9] makes use of the exponential mapping starting from an initial velocity  $v$  as indicated on the right side of (2), the variational method proposed in this paper directly relies on the definition of  $\text{dist}_M$  in the middle of (2).

### 2.3 Technical Issues

In this section, we will revisit a toolbox of functions that was presented in [9]. One important function that was used in [9], is the projection from an arbitrary function  $\vartheta \in L^2([0; 2\pi], \mathbb{R}) \supset \mathcal{C}$  onto the manifold. In [9, Section 3.2; Case 1] such a projection was elaborated. We will denote the projection by

$$P_\varepsilon : L^2([0; 2\pi], \mathbb{R}) \rightarrow \mathcal{C}_\varepsilon,$$

where

$$\mathcal{C}_\varepsilon := \Psi^{-1} \left( \left\{ r \left\| r - (2\pi^2, 0, 0)^\top \right\| < \varepsilon \right\} \right)$$

describes the manifold  $\mathcal{C}$  which is thickened by  $\varepsilon$ .  $\mathcal{C}_\varepsilon$  is an open subset of  $L^2([0; 2\pi], \mathbb{R})$ , and thus a manifold which contains  $\mathcal{C}$  as a submanifold.

We will also need the projection from the space  $L^2([0; 2\pi], \mathbb{R})$  on the tangent space  $T_\vartheta\mathcal{C}$  for any function  $\vartheta \in \mathcal{C}$ . This projection can be computed efficiently due to the small codimension of  $\mathcal{C}$  ( $= 3$ ) [9]. From now on, this projection will be denoted

$$P_\vartheta : L^2([0; 2\pi], \mathbb{R}) \rightarrow T_\vartheta\mathcal{C}.$$

To measure the distance of two given *shapes*  $\vartheta_1 \cdot \mathbb{S}^1$  and  $\vartheta_2 \cdot \mathbb{S}^1$ , the expression

$$\inf_{s_1 \in \mathbb{S}^1} \inf_{s_2 \in \mathbb{S}^1} \|\vartheta_1 \cdot s_1 - \vartheta_2 \cdot s_2\|_{L^2} = \inf_{s \in \mathbb{S}^1} \|\vartheta_1 - \vartheta_2 \cdot s\|_{L^2}$$

has to be calculated. The last equation holds since  $\mathbb{S}^1$  operates as an isometry on  $\mathcal{C}$ . Moreover, finding the minimizing  $s \in \mathbb{S}^1$  can be calculated via Discrete Fourier Transform [10]. Thus, this calculation needs only  $O(n \log(n))$  multiplications [2]. The function to calculate  $s \in \mathbb{S}^1$  given the preshapes  $\vartheta_1$  and  $\vartheta_2$  will be denoted  $\text{dft}_\mathcal{C} : \mathcal{C} \times \mathcal{C} \rightarrow \mathbb{S}^1$ .

### 3 Calculating Local Shape Morphings

In this section, two different algorithm to calculate geodesics between given shapes will be presented. Both algorithms will calculate the distance defined by (2). The first algorithm was presented by Klassen et al. [9] and uses a linearization of the exponential mapping. The second algorithm – proposed in this paper – will use the geodesic equation as gradient descent to minimize the functional  $E(m)$ .

#### 3.1 Morphing Via the Exponential Mapping

As we have seen, the following functional can be calculated efficiently using  $\text{dft}_\mathcal{C}$ .

$$H_{\vartheta_1}^{\vartheta_2}(f) = \inf_{s \in \mathbb{S}^1} \|\exp_{\vartheta_1}(f) - \vartheta_2 \cdot s\|_{L^2}^2, \quad f \in T_{\vartheta_1}\mathcal{C}. \quad (3)$$

The linearization of  $\exp_{\vartheta_1}(f)$  is explained in detail in [9]. The distance between the orbits  $\vartheta_1 \cdot \mathbb{S}^1 \subset \mathcal{C}$  and  $\vartheta_2 \cdot \mathbb{S}^1 \subset \mathcal{C}$  is the minimal  $\|f\|$  of any  $f$  that realizes the minimal value of  $H_{\vartheta_1}^{\vartheta_2}(\cdot)$ .

The above method has some important drawbacks. First of all, the numerical stability of  $\exp_\vartheta(\cdot)$  depends very much on the curvature at the point  $\vartheta$ . Hence, one expects an asymmetric runtime behavior, because the curvature of  $\mathcal{C}$  is heterogenous. In addition, the last operation that is calculated in (3) is the shape alignment via  $\text{dft}_\mathcal{C}$ . Hence, this method can get stuck in a local minimum. In Section 4 we will provide an example of this problem. One additional drawback is the runtime of this method. In the next section, we propose an alternative variational approach to compute geodesics which resolves all these drawbacks.

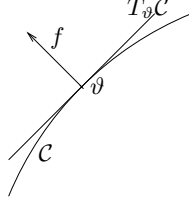


**Fig. 2.** A deformation  $f$  from a given preshape  $\vartheta$  is orthogonal to the tangent space  $T_{\vartheta}\mathcal{C}$  at this given preshape, iff the projection of the deformed preshape  $\vartheta + f$  onto the preshape manifold  $\mathcal{C}$  is equal to  $\vartheta$

### 3.2 Morphing Via the Geodesic Equation

Instead of restricting ourselves to the tangent space of a preshape  $\vartheta_1$  and trusting in the numerical stability of  $\exp_{\vartheta_1}(\cdot)$ , let us consider the entire path from  $\vartheta_1$  to  $\vartheta_2$ . With the help of the geodesic equation  $m''^{\text{tan}} \equiv 0$  it is easy to verify, whether a given path is a geodesic or not. Moreover, the geodesic equation guarantees an equidistant path and thus, a variational approach will take care of an online gauge fix.

If  $m$  fails to be a geodesic,  $m'$  is a non-parallel vector field along  $m$  and  $m''^{\text{tan}}$  measures the curvature of  $m$  within the manifold  $\mathcal{C}$ . Let us observe this measure in a discretized version of  $m$  in detail. The path shall be discretized in  $n \in \mathbb{N}$  equidistant preshapes. Each preshape shall be discretized in  $N \in \mathbb{N}$  points. Thus, a discretized path is

$$m^{N,n} := \left( m(0)^N, \dots, m\left(\frac{i}{n-1}\right)^N, \dots, m(1)^N \right) \in \mathbb{R}^{N \times n}, \text{ whereas}$$

$$\vartheta^N := \left( \vartheta(0), \dots, \vartheta\left(\frac{i}{N}\right), \dots, \vartheta\left(\frac{N-1}{N}\right) \right)^{\top} \in \mathbb{R}^N.$$

The discretized versions of  $P_{\varepsilon}$  and  $P_{\vartheta}$  will be known as  $P_{\varepsilon}^{\Delta}$  resp.  $P_{\vartheta}^{\Delta}$ . The vector field  $m'$  can be discretized by  $\frac{1}{n}m' \left( \frac{i+0.5}{n-1} \right) \approx m_{\cdot, i+1}^{N,n} - m_{\cdot, i}^{N,n}$  and the geodesic equation becomes

$$0 = P_{m_{\cdot, i}^{N,n}}^{\Delta} \left( \left( m_{\cdot, i+1}^{N,n} - m_{\cdot, i}^{N,n} \right) - \left( m_{\cdot, i}^{N,n} - m_{\cdot, i-1}^{N,n} \right) \right)$$

$$= -2P_{m_{\cdot, i}^{N,n}}^{\Delta} \left( m_{\cdot, i}^{N,n} - \frac{m_{\cdot, i-1}^{N,n} + m_{\cdot, i+1}^{N,n}}{2} \right).$$

Because of  $0 = P_{\vartheta}(f) \Leftrightarrow \vartheta \approx P_{\varepsilon}(\vartheta + f)$  (cf. Figure 2), we obtain the equation

$$m_{\cdot, i}^{N,n} = P_{\varepsilon}^{\Delta} \left( \frac{m_{\cdot, i-1}^{N,n} + m_{\cdot, i+1}^{N,n}}{2} \right). \quad (4)$$

Equation (4) can be interpreted as an iteration rule, that simulates the gradient descent and thus, moves a given path towards a geodesic. During this process the starting preshape  $m_{\cdot,1}^{N,n}$  and the target preshape  $m_{\cdot,n}^{N,n}$  aren't be altered. Thus, this process converges towards a geodesic from  $\vartheta_1$  to  $\vartheta_2$ . To calculate a geodesic from  $\vartheta_1$  to the orbit  $\vartheta_2 \cdot \mathbb{S}^1$ , we calculate a realignment in every iteration step. Our proposal for the iteration step is therefore<sup>3</sup>

```

Step 1: for (i=1; i<n-1; i++) {
     $m_{\cdot,i}^{N,n} := P_{\varepsilon}^{\Delta} \left( \frac{m_{\cdot,i-1}^{N,n} + m_{\cdot,i+1}^{N,n}}{2} \right)$ 
}
Step 2: for (i=1; i<n; i++) {
     $m_{\cdot,i}^{N,n} := m_{\cdot,i}^{N,n} * \text{dft\_C}(m_{\cdot,i}^{N,n}, m_{\cdot,i-1}^{N,n});$ 
}

```

By this extended iteration the starting preshape  $\vartheta_1$  remains fix but the target preshape  $\vartheta_2$  can be modified. This modification will only take place along the orbit  $\vartheta_2 \cdot \mathbb{S}^1$  and thus, the *shape* of  $\vartheta_2$  remains the target of the morphing.

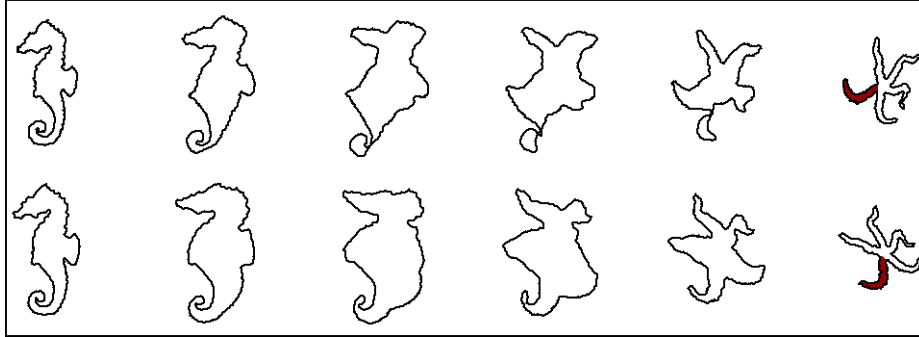
## 4 Benchmarking

To illustrate the difference between these two algorithms, we will discuss a specific morphing example. For this purpose, we have used the SQUID database of fish shapes [12]. In the first subsection, we will examine the morphing process between a seahorse and a starfish. This morphing will be done with a very high resolution ( $N = 500$  angles along each preshape;  $n = 300$  intermediate morphing steps). Specifically we show that the shooting method gets stuck in a local minimum, whereas the variational method calculates the global minimum with respect to shape realignments. In the second subsection we will analyze the speed of both algorithms for  $N = 500$  and  $n = 1, \dots, 100$ , showing in particular that our variational method computes minimas within seconds where the shooting method takes more than one hour.

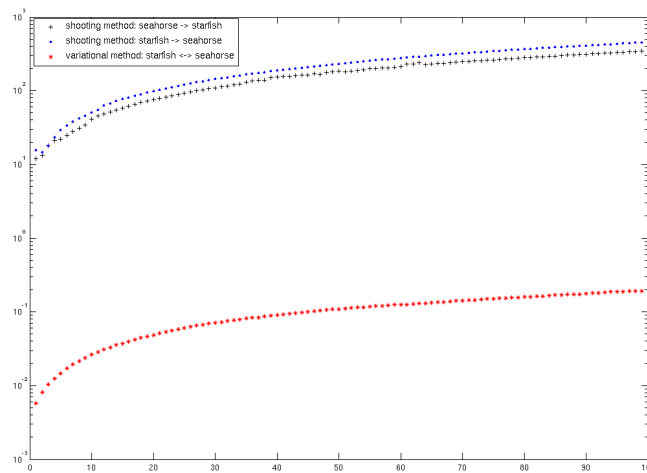
### 4.1 Dissimilarity of a Seahorse and a Starfish

Figure 3 shows the morphing of a seahorse towards a starfish. The first row shows the morphing according to the shooting method, whereas the second row shows the result of the variational method. Both are valid morphings of preshapes, but the calculated alignments are different in both algorithms. This leads to a self-intersection in the first case, whereas in the second case, the tail of the seahorse *unrolls* in an expected natural manner. This is due to the different alignments of the target shape. To emphasize the alignments, the same *region* of the target shape is colored. It's easy to see that the variational method moves the tip of the tail towards the tip of that region. Moreover, the first geodesic has the length 13.8, whereas the second geodesic has the length of 12.2. Therefore, the shooting method gets stuck in a local minimum.

<sup>3</sup> Note that each index starts at 0.



**Fig. 3.** The morphing of a seahorse towards a star fish is calculated via both algorithms. **First row:** The shooting method [9] gets stuck in a local minimum. **Second row:** Our variational method calculates the *global minimum* with respect to realignments. **Last column:** To illustrate the different alignments, the same region is colored in the target shape.



**Fig. 4.** Here the computation time to calculate geodesics is presented. The shapes are highly resolved and on the x-axis the discretization of the morphing is shown. The runtime via the variational method has two advantages. **Symmetry:** The geodesic calculation does not depend on the starting shape, whereas the runtime for the shooting method varies by ca. 25%. **Runtime:** The variational method is faster by a factor of 1000.

In this example, we used a discretization of  $N = 500$  for the preshapes. Therefore, there exist 500 different alignments for the target preshape. Calculating the geodesic distance between the preshapes with respect to all alignments, we could confirm that 12.2 is the global minimum with respect to preshape alignment. Thus, the calculation of realignments serves the purpose of finding the minimal distance between two given shapes.

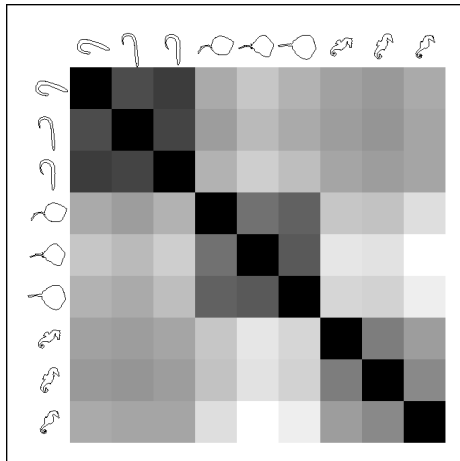
## 4.2 Computation Time

Figure 4 shows the computation time of both methods. It varies from the computation time in [9] because we use highly resolved preshapes and the methods stop only if they can provide a very accurate result. On the horizontal axis the discretization resolution of the geodesic is noted. For the shooting method this is the discretization of the exponential mapping. For the variational method this is the number of shapes that discretize the path on the manifold. First of all, we see that the computation time is not symmetric for the shooting method. Moreover, the computation time varies by 20 to 30 percent. This is due to the fact that the shooting method depends highly on the curvature at the starting shape. The variational method is symmetric and thus, the runtime does not depend on the starting shape. In addition, the calculation time is less than 100 milliseconds in the highly resolved case. If we use the same resolution as in [9], the variational method takes only a few milliseconds.

## 5 Conclusion

We presented a new variational approach to calculate geodesics in the shape space introduced in [9]. This shape space consists of  $S^1$ -orbits within a manifold. We start with an arbitrary parameterization of two given shapes and a path between these two *points of the manifold*. This path is then shortened via our variational method by alternating a two-step iteration process. The first step uses a gradient descent method and the second step realigns efficiently all preshapes along the observed path.

The proposed variational approach has several advantages over the shooting method used in [9]: Firstly, it is more stable since in contrast to the exponential



**Fig. 5.** The confusion matrix for a set of nine shapes

map, the variational method does not accumulate projection errors. Moreover, our gradient descent method provides an online gauge fix. Secondly, the formulation of the variational method does not rely on the starting shape, and thus the formulation of the metric is numerically symmetric. Thirdly, the calculation time is considerably smaller. In our examples, the calculation time typically improves by a factor of 1000. In addition, in our experiments our algorithm provides the *globally* optimal alignment between the given shapes. The practical implication of these drastic improvements in speed is that for a database of 100 shapes of high resolution, the confusion matrix consists of 4950 different entries and can be calculated in 8 minutes instead of 5 days<sup>4</sup>. Thus, the efficient use of this metric allows to cluster a considerable amount of shapes (cf. Figure 5). Future work will be focused on generalizing the concepts of geodesics on shape spaces to higher-dimensional shapes (e.g., surfaces).

## References

1. M. Bergtholdt and C. Schnörr. Shape priors and online appearance learning for variational segmentation and object recognition in static scenes. In *Pattern Recognition, Proc. of DAGM*. LNCS, Springer, 2005.
2. P. Bürgisser, M. Clausen, and M. A. Shokrollahi. *Algebraic Complexity Theory*. Grundlehren der Mathematischen Wissenschaften, Vol. 315. Springer-Verlag, 1997.
3. S. Chern, W. Chen, and K. S. Lam. *Lectures on Differential Geometry*. World Scientific, 1999.
4. D. Cremers, T. Kohlberger, and C. Schnörr. Shape statistics in kernel space for variational image segmentation. *Pattern Recognition*, 36(9):1929–1943, 2003.
5. D. Cremers and S. Soatto. A pseudo-distance for shape priors in level set segmentation. In N. Paragios, editor, *IEEE 2nd Int. Workshop on Variational, Geometric and Level Set Methods*, pages 169–176, Nice, 2003.
6. M. P. do Carmo. *Differential Geometry of Curves and Surfaces*. Prentice-Hall, 1976. 503 pages.
7. I. L. Dryden and K. V. Mardia. *Statistical Shape Analysis*. Wiley, Chichester, 1998.
8. E. Klassen and A. Srivastava. Geodesics between 3d closed curves using path-straightening. In *European Conference on Computer Vision (ECCV)*, volume 3951 of *LNCS*, pages 95–106, Graz, Austria, 2006. Springer.
9. E. Klassen, A. Srivastava, W. Mio, and S. H. Joshi. Analysis of planar shapes using geodesic paths on shape spaces. *IEEE Trans. Pattern Anal. Mach. Intell.*, 26(3):372–383, 2003.
10. J. S. Marques and A. J. Abrantes. Shape alignment – optimal initial point and pose estimation. *Pattern Recognition Letters*, 18(1):49–53, 1997.
11. P. Michor and D. Mumford. Riemannian geometries on spaces of plane curves. *J. of the European Math. Society*, 2003.
12. F. Mokhtarian, S. Abbasi, and J. Kittler. Efficient and robust retrieval by shape content through curvature scale space, 1996.

---

<sup>4</sup> Even at low resolution the shooting method needs more than one hour.